Spin Phonon Coupling in Hexagonal Multiferroic $YMnO_3$

S. Petit,[1] F. Moussa,[1] M. Hennion,[1] S. Pailhès,[1] L. Pinsard-Gaudart,[2] and A. Ivanov[3]

[1]*Laboratoire Léon Brillouin, CEA-CNRS, CE-SACLAY, F-91191 Gif sur Yvette, France*
[2]*Laboratoire de Chimie des Solides, URA 446 CNRS, Université Paris-Sud, Orsay, France*
[3]*Institut Laue langevin, 6, rue Jules Horowitz, BP 156 F-38042 Grenoble, France*

(Received 12 June 2007; published 28 December 2007)

Inelastic neutron scattering measurements have been performed on $YMnO_3$, aiming to study the interplay between spin and lattice degrees of freedom in this hexagonal multiferroic material. Our study provides evidence for a strong coupling between magnons and phonons, evidenced by the opening of a gap below T_N in the dispersion of the transverse acoustic phonon mode polarized along the ferroelectric axis. The resulting upper phonon branch is found to lock on one of the spin-wave modes. These findings are discussed in terms of a possible hybridization between the two types of elementary excitations.

DOI: 10.1103/PhysRevLett.99.266604 PACS numbers: 72.10.Di, 75.30.Ds, 77.22.Ej, 77.80.−e

Multiferroic $RMnO_3$ manganites (R is a rare earth) are examples of the very few systems whose ground state is characterized by coupled ferroelectric and magnetic orderings. While the possibility of using this coupling in novel electronic devices seems quite promising [1,2], the very nature of the interplay between magnetic ordering and ferroelectricity in these materials is at the moment one of the puzzling fundamental questions in the solid-state physics community.

As one moves along the $4f$ series, the decrease of the R-ion size induces a crystallographic change from an orthorhombic (R = Gd, Tb, Dy, ...) to a hexagonal (R = Ho, Y, Lu, ...) structure. Both are multiferroic but exhibit different kinds of multiferroicity [3]. In orthorhombic $RMnO_3$, magnetic frustration together with the spin-lattice coupling induced by the inverse Dzyaloshinski-Moriya (DM) interaction is thought to play a key role [3,4]. The magnetic frustration is due to competing exchange integrals between successive neighbors stabilizing incommensurate spiral magnetic phases [5]. The electric polarization appears right at the spiral ordering temperature T_N, via a uniform atomic displacement induced by the inverse DM interaction. The hexagonal $RMnO_3$ are likely to come under different physics. Indeed, the ferroelectric and magnetic orderings are no more concomitant since the electric polarization appears far above room temperature ($T_c \sim$ 900 K and $T_N \sim 100$ K). Nevertheless, evidence for a strong interplay between magnetic and ferroelectric order parameters has been shown by dielectric constant measurements, showing anomalies arising at T_N [6–8], diffraction techniques showing evidence for an enhancement of the electric moment below T_N [9]. More recently, various experiments as thermal expansion [10], thermal conductivity measurements [11], or Raman scattering [12] have pointed out the existence of a ''giant'' spin-lattice coupling that could be responsible for this interplay. Its microscopic origin remains, however, an open question.

To shed light on the spin-lattice coupling in hexagonal $RMnO_3$, we have undertaken inelastic neutron scattering measurements aiming to study both spin and lattice excitations. We have chosen the particular case of $YMnO_3$ since the absorption by yttrium is fairly low, as well as because the absence of crystal field excitations keeps clean the low energy range. Hexagonal $RMnO_3$ are formed by stacked Mn-O and R-O layers, the Mn ions being surrounded by three in-plane and two apical oxygen ions (MnO_5 bipyramide) and forming a triangular lattice (see Fig. 1). The ferroelectric distortion can be roughly understood as the combination of spontaneous tilting of the MnO_5 bipyramides along the O3O4 direction accompanied by a buckling of the Y-O planes. As a result, oxygen and yttrium atoms move off the hexagonal planes along **c** in opposite directions, giving rise to staggered ferroelectric moments. Since there are two O4 ions and only one O3 per Mn-O plane, the chemical unit cell finally acquires a nonzero net moment [13]. The Mn spins order antiferromagnetically below $T_N = 72$ K, the spins lying in the hexagonal plane, orthogonal to the Mn-O bonds as shown in Fig. 1 [14–18].

In this Letter, we report evidence for the opening of a gap, at low temperature in the dispersion of a transverse acoustic phonon mode. On the schematic picture of Fig. 1, this mode induces displacements of the various ions along the ferroelectric **c** axis. The wave propagates along $\mathbf{a}^*$ which is exactly the O3O4 tilting direction involved in the ferroelectric distortion. This particular phonon mode is thus closely related to ferroelectricity. Since this gap opens below T_N, it has to be due to some coupling with the magnetic subsystem. Locking of the resulting upper phonon branch on one of the spin-wave modes tends to support this idea.

High quality $YMnO_3$ single crystals of about 0.4 cm^3 have been grown using the standard floating zone technique. The neutron scattering experiments have been carried out on cold and thermal triple axis spectrometers at the Orphée-LLB reactor and at the Institut Laue Langevin. In all experiments, the crystal was placed in a closed-cycled refrigerator and oriented such that wave vectors in the form $(q, 0, \ell)$ reduced lattice units could be accessed in the horizontal scattering plane. Bent or flat pyrolytic graphite

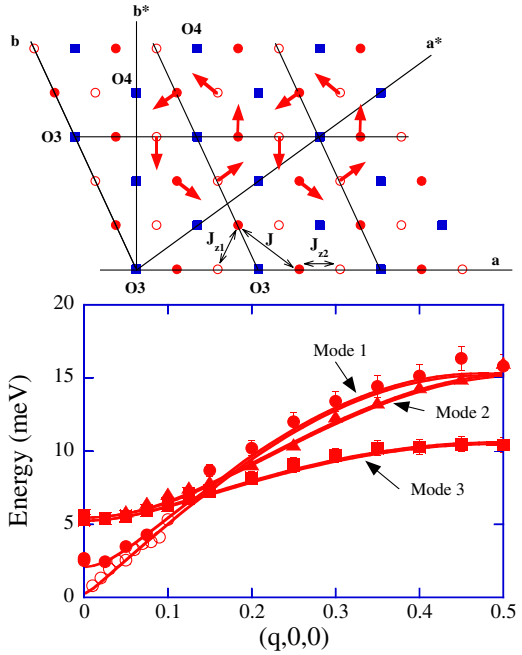

FIG. 1 (color online). Upper panel: schematic view of spin ordering and atomic positions in $YMnO_3$. The squares depict oxygen O3 and O4 positions, while the circles indicate Mn ones (filled and open symbols correspond, respectively, to the $z = 0$ and the $z = 1/2$ plane). The magnetic and chemical unit cell are identical with lattice parameters $a = 6.14$ Å and $c = 11.39$ Å. Lower panel: measured magnon dispersions along $\mathbf{a}*$. Solid lines are fits to the data according to the Heisenberg model (see the text). Mode 1 (closed circles) has been measured around (100) where it corresponds to out-of-plane fluctuations. The open circles correspond to the same branch measured around the (101) Brillouin zone. The decrease of the zone center gap is due to exchange along the $\mathbf{c}$ direction. Modes 2 and 3 (triangles and squares, respectively) have been measured around (006) where they correspond to in-plane fluctuations.

and Cu crystals were used as the monochromator and the analyzer, respectively, depending on the desired resolution, while open collimations were used to fully benefit from the focusing effects.

The spin dynamics have been studied by collecting constant-$\mathbf{Q}$ scans at different temperatures, leading to the spin-wave dispersions reported in Fig. 1. Our data are well described by the following spin Hamiltonian: $\mathcal{H} = \sum_{R,R',i,j} J_{R,i,R',j} \vec{S}_{R,i} \vec{S}_{R',j} + H \vec{S}_{R,i} . \vec{n}_i + D S^z_{R,i} S^z_{R,i}$, where $\vec{S}_{R,i}$ denotes the spin at magnetic site i in the cell R, $\langle \vec{S}_{R,i} \rangle$ is its mean value, and $\vec{n}_i = \frac{\langle \vec{S}_{R,i} \rangle}{|\langle \vec{S}_{R,i} \rangle|}$. $J_{R,i,R',j}$ describes the (scalar) exchange interactions, while H and D correspond to easy-axis and easy-plane anisotropies, respectively. In the linear spin-wave approximation, a good agreement is obtained with an antiferromagnetic interaction between in-plane nearest neighbors $J = 2.3$ meV, an easy-plane anisotropy $D = 0.33$ meV, and a particularly small easy-axis parameter $H = 0.0008$ meV. These measurements mainly confirm the results reported in [19–21]. However, detailed comparison of the neutron intensities with calculations of the magnetic dynamical structure factor based on the model discussed above enabled us to improve the understanding of the spin excitations in this frustrated system. First, we conclude that the exchange couplings J_{z1} and J_{z2} (see Fig. 1), that are responsible for the decrease of the 2.5 meV gap observed around (100) down to 0.28 meV around (101), are both ferromagnetic. Fitting to the data provides the following values, $J_{z1} = -0.025$ meV, as well as an estimation of $J_{z2} \sim -0.016$ meV. Next, the calculations enabled us to predict the polarization of the spin waves. Indeed, the in-plane or out-of-plane nature of the spin fluctuations induces modulations of the neutron intensities as a function of Q. This information was used to choose the best experimental conditions able to reveal properly each different mode. This enabled us to distinguish the high energy spin-wave modes 1 and 2 unresolved in [20].

We now turn to the description of the particular transverse phonon mode mainly polarized along the ferroelectric $\mathbf{c}$ axis and propagating along $\mathbf{a}^*$. Its dispersion was studied thanks to constant-$\mathbf{Q}$ scans performed at $(q, 0, 6)$ and $(q, 0, 12)$ with thermal as well as cold neutrons. The upper panel of Fig. 2 shows the dispersion of this transverse acoustic mode obtained at 200 K, as well as the dispersion of a roughly flat optic mode (see the squares and the triangles in the upper panel of Fig. 2). The optic mode energy is of about 18 meV (145 cm^{-1}), in good agreement with the Raman experiments reported in [22]. Below T_N the different spin-wave branches give rise to strong magnetic scattering discussed above. As shown in middle panel of Fig. 2, this signal is strong enough to hide the acoustic phonon mode beyond $q = 0.15$, except at small q (see the dotted line). Taking advantage of the decrease of the magnetic form factor as a function of $|\mathbf{Q}|$, the measurements around $(q, 0, 12)$ (lower panel) allow us to fully eliminate the magnetic scattering and thus to reveal the complete dispersion of the acoustic phonon mode. A close examination of the region around $q_o \sim 0.185$, $\omega \sim 6$ meV shows that the acoustic phonon dispersion exhibits at low temperature a gap around $\mathbf{q_o} = q_o \mathbf{a}^*$. It is accompanied by the expected intensity balance between the lower and the upper branch. This phenomenon can be clearly observed in Fig. 3 which shows the data obtained at $q = 0.15$, $q = 0.175$, and $q = 0.2$. Bringing together the different measurements as well as the fitted spin waves, we obtain the low temperature dispersions shown in the upper panel of Fig. 2. Further examination shows that the spin-wave mode 3 and the upper acoustic phonon branch essentially coincide around $\mathbf{q_o}$. The closure of the gap was studied by following the same experimental procedure at different temperatures up to 200 K. We report in the lower panel of Fig. 3 the energy ω_q of the most intense phonon branch determined for different q values. For values well below or well above q_o, no significant evolution of ω_q is observed up to 200 K. On the contrary,

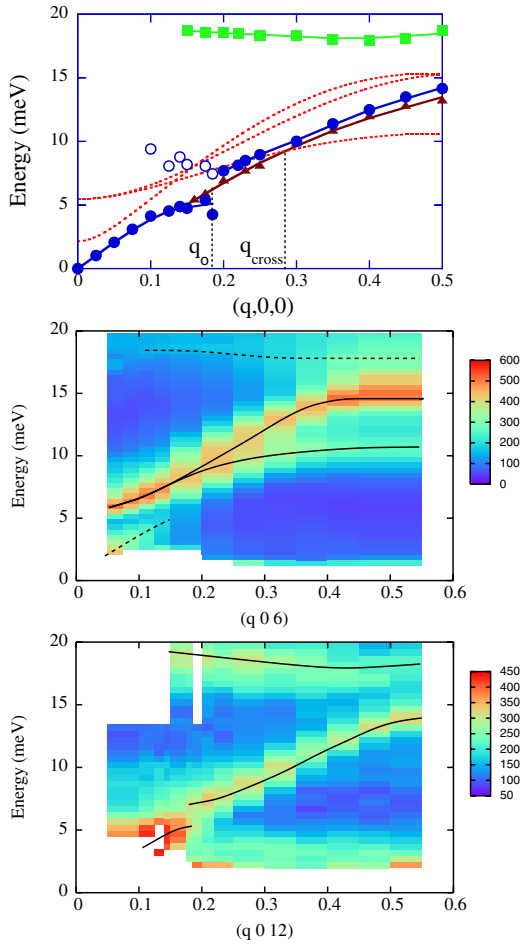

FIG. 2 (color online). Upper panel: phonon dispersions obtained at 200 K (triangles) and 18 K (circles). Closed and open symbols correspond to large and small intensities, respectively. The squares correspond to the optic phonon mode. Dotted (red) lines are calculated spin-wave dispersions. The gap in the phonon dispersion opens at $q_o \sim 0.185$. Crossing of the 200 K phonon dispersion with the spin-wave mode 3 arises at $q_{\text{cross}} \approx 0.3$ Lower panel: color mappings of the neutron intensity obtained as a function of energy transfer and wave vector $\mathbf{q} = q\mathbf{a}^*$ and taken around (0, 0, 6) and 18 K (middle panel) and (0, 0, 12), $T = 18$ K (lower panel). Solid and dashed lines are guides to the eyes.

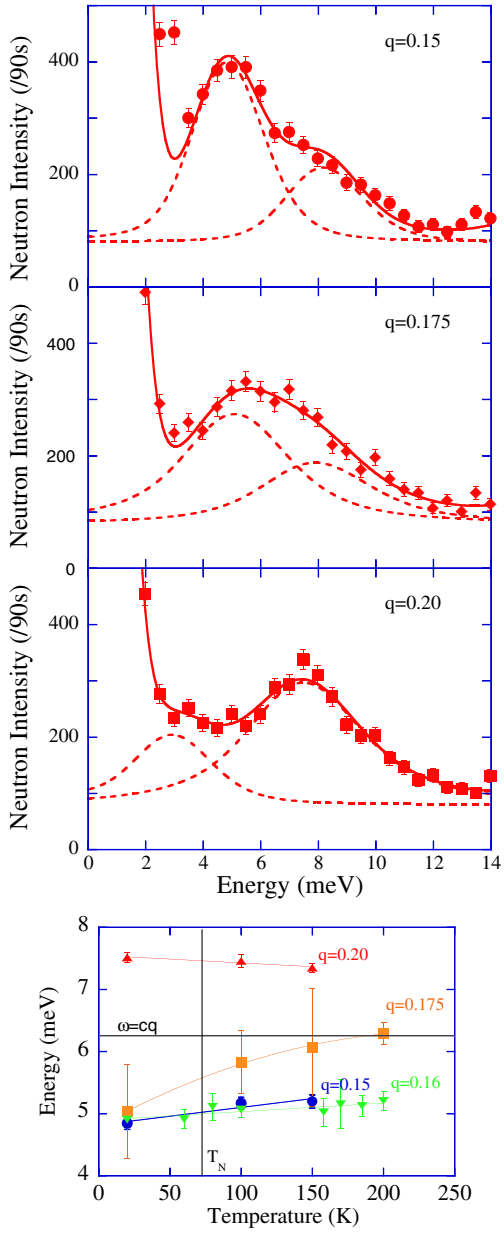

FIG. 3 (color online). Neutron intensity obtained at 18 K at (q, 0, 12) with $q = 0.15$, $q = 0.175$ and $q = 0.2$. The intensity balance is observed between modes at 5 meV and 7.5 meV. Evolution of the phonon energy as a function of temperature for the different q-values surrounding q_o: upward triangles, squares, circles and downward triangles correspond, respectively, to $q = 0.20$, $q = 0.175$, $q = 0.16$ and $q = 0.15$. The dotted line shows the phonon energy value at $q = 0.175$ expected for a linear acoustic dispersion.

the energy corresponding to $q = 0.175$ slightly increases from 5 to about 6 meV at 150 K. This is the value expected for a standard linear dispersion deduced from ω_q determined at $q = 0.15$ and $q = 0.20$. From this temperature dependence, we conclude that the gap opens mainly below T_N, showing its connection with the magnetic subsystem.

Some clues in the interpretation of these data can be found by considering, for example, similarities of the present experiments with the case of ferrous halides [23]. Indeed, in these materials, a valuable interpretation of both anomalous behavior of the thermal conductivity [24] and neutron scattering data [25,26] has been proposed on the basis of single-ion magnetostriction, arising from modulation of the crystalline field by the motion of nonmagnetic ions [27]. The corresponding interaction term reading as $V = g\sum_{\alpha,\beta,R,i} \epsilon_{R,i}^{\alpha,\beta} S_{R,i}^{\alpha} S_{R,i}^{\beta}$ couples the spins and the atomic displacements $u_{R,i,\alpha=x,y,z}$ via the local deformation $\epsilon_{R,i}^{\alpha,\beta} = \frac{\partial u_{R,i,\beta}}{\partial r_\alpha} + \frac{\partial u_{R,i,\alpha}}{\partial r_\beta}$. In turn, V is linear in the a_q^+ (creation) and a_q (annihilation) phonon operators. Because of the coupling between off diagonal spin components, V contains as

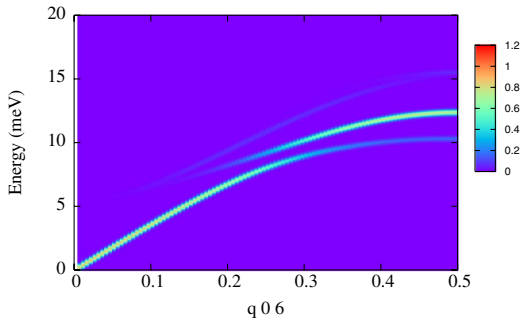

FIG. 4 (color online). Nuclear dynamical structure factor (in arbitrary units) calculated as a function of energy and wave-vector along $(q, 0, 6)$ for $g = 0.03$.

well linear terms in the spin-wave operators. In the magnetically ordered phase, these linear terms are known to give rise to a resonant interaction and in turn to the hybridization of the phonon and the spin waves [24,28]. For simplicity, we consider here only the coupling with the studied transverse phonon branch and obtain the following Hamiltonian: $\mathcal{H}' = \mathcal{H} + \Omega_q a_q^+ a_q + V$, where Ω_q corresponds to the 200 K phonon dispersion deduced from experiments. The model basically predicts the hybridization between the phonon and the spin-wave mode 3. This results in the emergence of magnetoelastic modes, separated by a gap opening at the crossing point between the bare dispersions, namely, at $q_{\text{cross}} \approx 0.3$. Figure 4 shows a calculation of the nuclear dynamical structure factor revealing the phononlike component of the hybrid excitations. In principle, it can be directly compared with the neutron data shown in the lower panel of Fig. 2. The calculation shows a jump from the lower to the upper mode, providing a natural interpretation for the experimentally observed gap. The main difference, which is not understood so far, comes from the value of the wave vector q_o which is slightly smaller than the theoretical q_{cross}. Note that the strong reduction around T_N of the thermal conductivity reported by [11] could be explained by this model, as is the case in ferrous halides [24].

The possible existence of hybridized excitations has also been reported very recently in orthorhombic $GdMnO_3$ and $TbMnO_3$ [29]. These authors have interpreted their infrared spectroscopy measurements in terms of "electromagnons," hybridized magnetic and phononic low energy excitations (at 20 cm^{-1} or 2.48 meV). This result, together with the analysis given in [30], agrees with the neutron study by Senff *et al.* [31], which identifies the electromagnon with a spin-wave mode observed at the same energy. These authors tentatively attribute this excitation to the Goldstone mode of the multiferroic phase. In the present hexagonal case, the situation is, however, quite different since the hybridization results from the resonant interaction between two boson modes. It should be mentioned, however, that the DM interaction invoked in the physics of orthorhombic $RMnO_3$ can lead also to this resonant interaction. This would provide an overall picture but specific theoretical work is necessary to clarify this issue.

In summary, besides the detailed study of the spin wave branches in $YMnO_3$, our neutron experiments provide evidence for the opening of a gap below T_N around $\mathbf{q_o} = 0.185\mathbf{a}^*$ in the dispersion of the transverse acoustic phonon mode polarized along the **c**-ferroelectric axis. The upper phonon branch is found to lock on one of the spin-wave modes. These data reveal that a strong coupling between spins and phonons is at play in this hexagonal multiferroic material. These findings are discussed in terms of a possible hybridization between the two types of elementary excitations.

We would like to thank C. Lacroix and Y. Sidis for fruitful discussions.

[1] M. Fiebig *et al.*, J. Phys. D **38**, R123 (2005); M. Fiebig *et al.* Nature (London) **419**, 818 (2002).
[2] T. Kimura *et al.*, Nature (London) **426**, 55 (2003).
[3] S. W. Cheong and M. Mostovoy, Nature Mater. **6**, 13 (2007).
[4] I. A. Sergienko and E. Dagotto, Phys. Rev. B **73**, 094434 (2006).
[5] M. Kenzelmann *et al.*, Phys. Rev. Lett. **95**, 087206 (2005).
[6] Z. J. Huang *et al.*, Phys. Rev. B **56**, 2623 (1997).
[7] N. Iwata *et al.*, J. Phys. Soc. Jpn. **67**, 3318 (1998).
[8] F. Yen *et al.*, Phys. Rev. B **71**, 180407(R) (2005).
[9] S. Lee *et al.*, Phys. Rev. B **71**, 180413(R) (2005).
[10] C. de la Cruz *et al.*, Phys. Rev. B **71**, 060407(R) (2005).
[11] P. A. Sharma *et al.*, Phys. Rev. Lett. **93**, 177202 (2004).
[12] P. Litvinschuk *et al.*, J. Phys. Condens. Matter **16**, 809 (2004).
[13] T. Katsufuji *et al.*, Phys. Rev. B **66**, 134434 (2002).
[14] E. F. Bertaut *et al.*, Phys. Lett. **5**, 27 (1963).
[15] A. Munoz *et al.*, Phys. Rev. B **62**, 9498 (2000).
[16] M. Fiebig *et al.*, Phys. Rev. Lett. **84**, 5620 (2000).
[17] M. Janoschek *et al.*, J. Phys. Condens. Matter **17**, L425 (2005).
[18] D. Kozlenko *et al.*, JETP Lett. **82**, 193 (2005).
[19] T. J. Sato *et al.*, Phys. Rev. B **68**, 014432 (2003).
[20] J. Park *et al.*, Phys. Rev. B **68**, 104426 (2003).
[21] O. P. Vajk *et al.*, Phys. Rev. Lett. **94**, 087601 (2005).
[22] M. N. Iliev *et al.*, Phys. Rev. B **56**, 2488 (1997).
[23] M. T. Hutchings *et al.*, J. Phys. C **3**, 307 (1970).
[24] G. Laurence *et al.*, Phys. Rev. B **8**, 2130 (1973).
[25] W. B. Yelon *et al.*, Solid State Commun. **15**, 391 (1974).
[26] K. R. A. Ziebeck *et al.*, in *Proceedings of the Conference on Neutron Scattering, Gatlinburg, TN, 1976*, edited by R. M. Moon (National Technical Information Service, Springfield, VA, 1976).
[27] K. Kawasaki *et al.*, Prog. Theor. Phys. **29**, 801 (1963).
[28] S. W. Lowesey, J. Phys. C **5**, 2769 (1972).
[29] A. Pimenov *et al.*, Nature Phys. **2** 97 (2006).
[30] H. Katsura *et al.*, Phys. Rev. Lett. **98**, 027203 (2007).
[31] D. Senff *et al.*, Phys. Rev. Lett. **98**, 137206 (2007).